Chapter 1

Introduction

1.1 General

The DLVO theory (1,2) states that the total force (F_t) between lyophobic particles immersed in a solvent is given by the algebraic sum of the electrical double layer repulsion (F_e) and the van der Waals (vdW) attraction (F_d):

$$F_t = F_e + F_d \tag{1}$$

Figure 1.1 shows a schematic of the interaction between two surfaces in a polar liquid. Mathematically, F_e can be approximately described by an exponential function, whereas F_d follows an inverse power law. The net result is that, usually, at small separations, the dispersion force dominates, whereas, at larger separations, the double layer repulsion is dominant. This interplay between the two forces gives rise to a typical curve with an energy barrier as shown in Figure 1.

With the advent of force measuring devices like the Surface Force Apparatus (SFA) and the Atomic Force Microscope (AFM), it has become possible to measure, with great sensitivity, the interaction forces between two surfaces down to molecular separations. As a result of these force measurements, serious limitations of the DLVO theory have come into light. Specifically, in aqueous solutions, depending on the situation, one has to take into account: (i) the extraneous attraction between hydrophobic surfaces known as the hydrophobic force (3-5); (ii) repulsive primary hydration forces between lipid bilayers (6) and silica surfaces (7-11); (iii) repulsive secondary hydration forces between mica and rutile surfaces (12,13); (iv) oscillatory forces due to solvent structure and layering near surfaces (14,15); (v) depletion force in micellar systems (16,17); (vi) ion-correlation effects (18) and (vii) fluctuation forces between soft surfaces like bilayers (19).

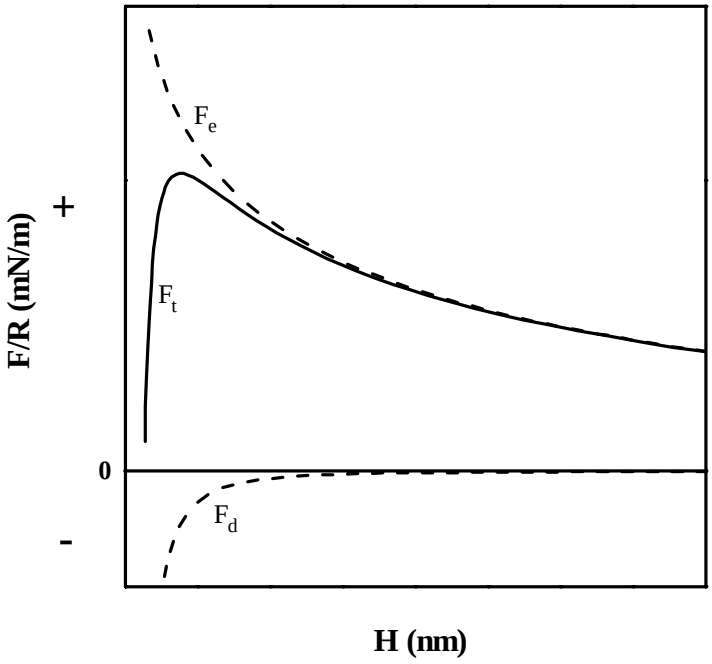

Figure 1.1 A typical DLVO curve. The upper and lower dashed lines represent the electrical (F_e) and van der Waals (F_d) forces respectively. The solid line represents the total interaction force (F_t), which, according to the DLVO theory, a sum of F_e and F_d.

Considerable theoretical work has been done in the past in an attempt to understand the origin of these non-DLVO forces. Nevertheless, two of the most widely debated topics in the field of surface forces today are the origins of hydration and hydrophobic forces. These forces are extremely important since not only do they dictate the stability of aqueous colloidal suspensions, but also control processes like the dynamics of molecular self-assembly, transformation of biological membrane assemblies, protein folding, cell fusion, wetting, froth flotation, deinking and adhesion.

1.2 Direct Measurement Techniques for Hydration and Hydrophobic Forces

1.2a. The Surface Forces Apparatus (SFA)

Shown in Figure 1.2 is a schematic of the SFA, which is widely used for force measurements in both polar and nonpolar solvents. This apparatus was devised by Israelachvili and Adams (20) and is based on an apparatus that was used earlier by Tabor and Winterton (21) for the measurement of vdW forces between mica sheets in air or vacuum. Cleaved mica sheets (1-4 μm thick), with back surfaces silvered, are glued to glass half cylinders, forming molecularly smooth surfaces of cylindrical geometry. The cylinders are arranged in a crossed cylinder geometry, that is, the axes of the cylindrical surfaces are arranged to cross at 90^{o}. One of the surfaces is mounted on a double cantilever spring. This spring arrangement increases the torsion stiffness of the spring dramatically, ensuring that twisting motions are negligible. The other surface is mounted on a tubular piezoelectric crystal. The surfaces are brought towards each other using the piezo and white light is directed from the bottom. The tubular shape of the piezo allows light to pass through, which is then focused into a spectrometer. In the spectrometer, the light appears as fringes which are called FECO fringes. This method enables the detection of the separation between the surfaces to an accuracy of 0.2 nm.

Now, when the two cylindrical surfaces approach each other, the spring holding the lower surface deflects in response to the DLVO forces. The magnitude of the spring deflection (X) can be determined from the difference between the piezo displacement and the change in the surface

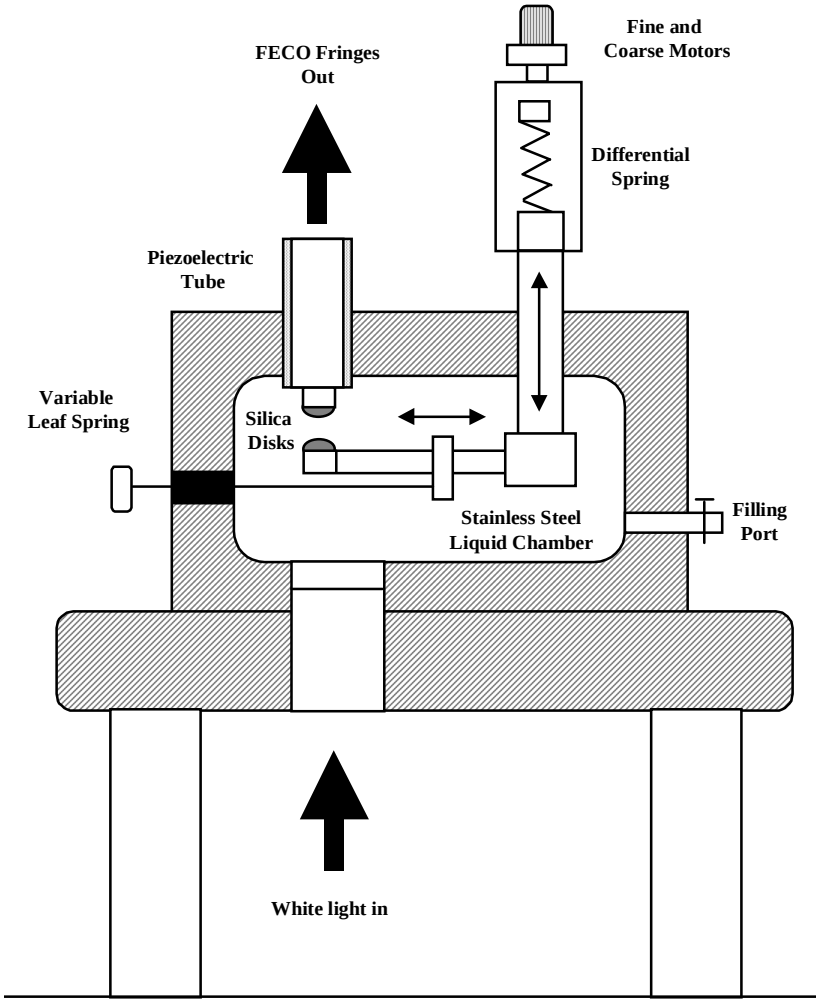

Figure 1.2 Schematic representation of the Mark IV Surface Forces Apparatus

separation (as seen from the FECO fringes). Knowing the spring constant (k), the force (F_t) can be calculated from the Hooke's law, $F_t=kX$. It should be mentioned that at separations where the gradient of the force exceeds k, the two surfaces jump into contact. This is the basis of another method used by various investigators for force measurement, known as the jump method, where k is changed and the jump distance recorded. This gives the gradient of the force, which can now be recorded as a function of the separation.

One of the advantages of the SFA over the AFM is that the stiffness of the springs in SFA can be changed *in situ*. Also, the separation distances can be monitored to a greater accuracy by this technique. This technique also allows one to monitor certain important factors like the adsorption layer thickness, viscosity and refractive index. The main disadvantage of this apparatus is that it can only use transparent samples like mica, although silica (9) and alumina-coated mica surfaces (22,23) have been used successfully. However, this can be overcome by using a piezoelectric bimorph to detect the surface separation instead of interferometry. This has been successfully used by Parker (24) to measure the forces between glass surfaces.

1.2b The Atomic Force Microscope (AFM)

In the late 1980s, the development of the AFM as a force measuring device enabled measurement of surface forces with remarkable sensitivity $>10^{-10}$N. This method was pioneered by Ducker *et al.* (25) who modified the AFM for force measurements by gluing a glass microsphere to the tip of the cantilever and measured the forces between the sphere and a flat silica surface in water. This technique is shown schematically in figure 2.3. The flat surface is mounted on a piezo crystal, which controls the separation between the sphere and the plate. The deflection of the spring is monitored by an optical lever technique, in which a laser beam is focussed on the back of the cantilever. The reflected beam is directed onto a split or quadrant photodiode via a mirror. Any deflection of the spring results in the light spot moving vertically across the face of the photodiode, leading to a voltage change at each half of the diode.

The biggest advantage of the AFM is that it allows force measurements between opaque materials. Thus, the AFM has been used to measure forces between polypropylene (26),

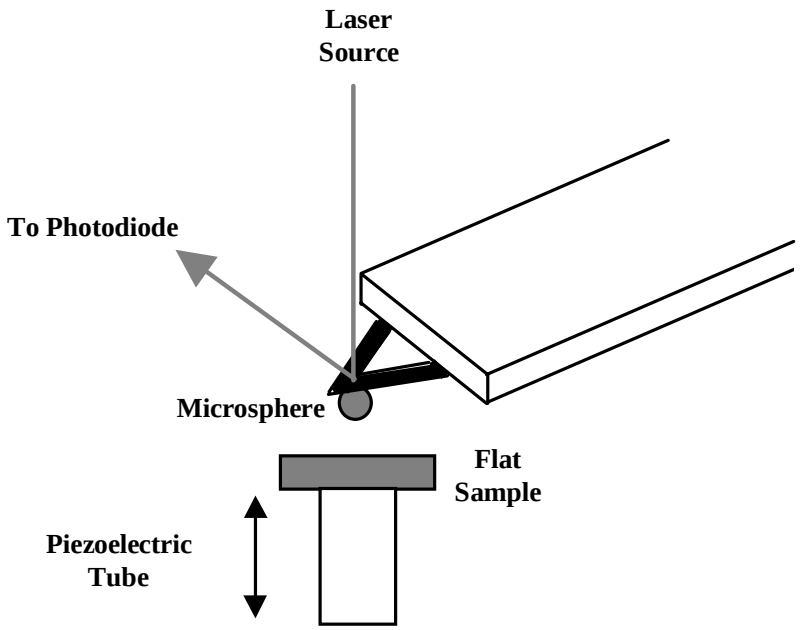

Figure 1.3 Schematic representation of the Atomic Force Microscope (AFM) used to measure the force on a micro sphere.

polystyrene (27), gold (28,29), ZnS (30), covellite (31) and zirconia (32). The drawbacks of the AFM when compared to the SFA are: (i) Zero separation distance cannot be established accurately. This makes determination of the adsorbed layer thickness impossible. (ii) Spring constant cannot be varied in situ. (iii) the adhesion force cannot be measured reliably since the springs undergo torsion before separation.

1.3 The Hydrophobic Force

Israelachvili and Pashley (3) used the SFA to measure, for the first time, the hydrophobic force between two mica surfaces in aqueous solutions of cetyltrimethylammonium bromide (CTAB). This extraneous attraction was observed at separation distances less than 10 nm and could be described by an empirical single exponential force law as follows:

$$F_h/R = -C_o\exp(-H/D_o) \qquad (2)$$

where R is the mean radius of interaction of the interacting bodies, C_o is a preexponential factor and D_o is called the decay length. By fitting their force data, Israelachvili ad Pashley obtained values of 30 mN/m and 1.2 nm for C_o and D_o respectively. During the last 15 years, the existence of this force has been confirmed independently by various other research groups (4,5,33,34). The hydrophobic force has been measured using different force measuring devices like AFM, the Light Lever Instrument for Force Evaluation (LLIFE) (35), and the bimorph-SFA (24). It has also been observed between a variety of surfaces like hydrophobized silica (4) and gold (28), polypropylene (26), polystyrene (27).

There is considerable debate in literature over the range and magnitude of the hydrophobic force. Investigators also disagree over the exact functional form of the hydrophobic force. Some suggest (3,34) that, empirically, the hydrophobic force may be represented using Eq.[2], while others (5) propose that a double exponential function as shown below is probably more accurate:

$$\frac{F_{hyd}}{R} = C_1 \exp\left(\frac{-H}{D_1}\right) + C_2 \exp\left(\frac{-H}{D_2}\right) \quad (3)$$

Still others (36,37) have proposed that the hydrophobic force can be expressed in the form of a power law, similar to the van der Waals force:

$$F_h/R = -K_{131}/6H^2 \quad (4)$$

where K_{131} represents the interaction constant between two surfaces **1** across a medium **3**. Nevertheless, no single functional form has found universal acceptance.

The most intensely debated aspect of the hydrophobic force, however, may be its origin. Any proposed theory, of course, must satisfactorily explain all the experimental observations. This is not easy since contradictory trends in the hydrophobic force have often been reported in literature. Consider for example, the effect of electrolyte on the hydrophobic force. Experiments indicate that the attraction may increase (38), decrease (39,40) or remain constant (26) in the presence of electrolyte. Similarly, experiments conducted to study the effect of temperature on the hydrophobic attraction have shown two different trends-in one case the force was observed to reduce at higher temperatures (41), while in another the opposite occurred (24). In addition to the two factors listed above, hydrophobic forces have been observed to be strongly dependent on factors like the method of preparation of the hydrophobic substrate, stability of the hydrophobic layer, degree of ordering in the layer, hydrophobicity (as estimated by the contact angle) and presence of dissolved gas. In the following sections, we will briefly review the literature on some experimental measurements of the hydrophobic force and also examine the various theories proposed for the origin of this mysterious attraction.

1.3a *Experimental Evidence for the Hydrophobic Force*

This section has been organized according to the methods of preparation of the hydrophobic surface since it has been observed that the range and magnitude of the hydrophobic forces are sharply dependent on them. Five different methods of preparation have been

considered: (i) self assembly from aqueous solutions, (ii) self-assembly from non-aqueous solutions, (iii) L-B deposition, (iv) chemically modified surfaces and (v) naturally hydrophobic surfaces.

(i) Self-Assembled Monolayers (SAMs)

As mentioned earlier, the first measurement of hydrophobic force was made by Israelachvili and Pashley (3) using cylindrical mica surfaces rendered hydrophobic by adsorption of CTAB from solution. Then the decay length (D_o) of the measured hydrophobic force was noted to be 1.0 nm (3). The contact angle of the hydrophobized mica surface was ~64^o. Pashley (42) reinvestigated the forces between bilayers of CTAB on mica and concluded that the surfactant sample used in the earlier investigation was probably contaminated. Kekicheff et al. (43) remeasured the forces between mica surfaces in CTAB solutions and found that in the concentration regime of 3-7x10^{-6}, the mica surfaces are nearly neutralized and exhibit a hydrophobic force with D_o ~2.5 nm. The θ_a of the CTAB coated mica surfaces at these conditions was ~94^o.

Herder (44) measured the hydrophobic forces between mica surfaces in solutions of dodecylammonium hydrochloride (DAHCl) and octylammonium hydrochloride (OAHCl). The mica surfaces exhibited a θ_a of approximately 90^o and the D_o value was observed to be the same as that measured between CTAB coated mica surfaces by Israelachvili and Pashley (3). Parker et al. (45) measured the surface forces between glass surfaces in CTAB solutions and observed that at a concentration of ~5x10^{-5}M, the surfaces are almost neutralized. Further, at these conditions, net attractive force were observed which extended out to separation distances of ~15 nm. Thus, the hydrophobic forces between SAMs on mica and silica are in general observed to be short ranged, i.e., their effect extends to a maximum separation distance of ~10 nm and the decay lengths are in the range of 1-2 nm. As will be seen shortly, this range is much less than those for surfaces hydrophobized by other methods.

There are, however, special conditions under which relatively long range hydrophobic forces between SAMs on mica and silica may exist. Yoon and Ravishankar (46) measured the

hydrophobic forces between mica surfaces in the solutions of dodecylammonium hydrochloride (DAHCl) and a neutral surfactant-octanol. At $5x10^{-6}$M DAHCl and $5x10^{-7}$M octanol, net attractive forces were observed which could be fitted to Eq.[2] with D_2=6.8 nm. In this case, hydrophobic forces could be detected at separations as large as 30 nm. The large hydrophobic force was attributed to the fact that octanol may coadsorb in the monolayer of dodecylammonium ions on mica, thereby, increasing the packing density of hydrocarbons on the surface and making it more hydrophobic. Similarly, both Yoon and Ravishankar (73) and Rutland *et al*. (47) measured the hydrophobic forces between mica surfaces in DAHCl solutions at alkaline pHs where the concentration of the neutral dodecylamine (DA) reaches a maximum. It was observed that, at such pHs, the coadsorption of DA makes the DAH^+ monolayer more compact, thereby resulting in a longer range hydrophobic force. More recently, Craig *et al*. (35) reported that the hydrophobic interaction between CTAB-coated silica surfaces may extend out to separations larger than 50 nm. The reason for the appearance of such long-range forces is, however, unclear.

(ii) SAMs from non-aqueous solutions

Tsao *et al*. (41) deposited monolayers of dihexadecylammonium (DHDA), dioctadecyldimethylammonium (DODA) and dieicosyldimethylammonium (DEDA) on mica from solutions of cyclohexane. The hydrophobic forces between such monolayers were observed to be very long ranged (D_2~25 nm). However, the strength of the attraction between two DHDA monolayers was much lower than those between two DEDA or DODA monolayers. To explain this, the authors studied the AFM images of these surfactants on mica and observed that monolayers of the latter are crystalline whereas those of the former are amorphous. It was proposed that this is because the chain melting temperature (T_c) of DHDA is close to the ambient temperature, whereas those of DODA and DEDA are much higher. It was suggested that the state of the monolayers may be the reason why the hydrophobic force between DHDA monolayers are weaker. Further, it was observed that when the temperature is increased to values close to T_c, the hydrophobic force decreases. This was attributed to the fact that at T_c the hydrocarbon chains in the monolayer may melt leading to a decrease in the crystalline order. Later, Rabinovich and Yoon (48) quantified the order of the hydrocarbon chains in DODA

monolayers using an order parameter, *S*, obtained from FTIR measurements. The authors found a linear relationship between the values of *S* and the hydrophobic force parameters obtained by Tsao *et al*.

(iii) Langmuir Blodgett Monolayers (LB)

Claesson *et al*. (36) conducted force measurements between L-B monolayers of dimethyldioctadecylammonium bromide (DDOAB) on mica. The surfaces exhibited a θ_a of ~94^o and the measured forces could be represented by a double-exponential function with D_1=1.2 nm and D_2=5.5 nm. Claesson and Christenson (5) measured the hydrophobic forces between L-B monolayers of the same surfactant deposited at a lower surface pressure, and obtained very long-range hydrophobic forces extending out to approximately 90 nm. Also, these authors showed convincingly that the hydrophobic force indeed follows a double-exponential force law with D_1=2-3 nm and D_2=13-16 nm. Very recently, Hato (50) conducted force measurements between surfaces of controlled hydrophobicity. Mica surfaces were coated with mixed L-B layers exposing different amounts of hydrophobic (CH_3CH_2-) and hydrophilic ($HOCH_2$-) groups to the aqueous phase. It was observed that the short-range part of the hydrophobic force shows a relationship with the hydrophobicity (contact angle) of the surface, whereas the long-range does not.

In general, the force measurements conducted to date suggest that L-B deposited monolayers exhibit a much longer-range hydrophobic force than SAMs, and the D_2 values obtained are usually in the range of 15-20 nm. Nevertheless, two particular experiments require special mention. Kurihara and Kunitake (51) conducted force measurements between L-B layers of a polymerized ammonium amphiphile on mica, which gave θ_a in the range 84^o-94^o. The authors observed exceptionally long-range hydrophobic forces extending upto 300 nm, which could be fitted to D_2 values greater than 60 nm. However, these layers were not L-B deposited in the conventional up-stroke motion, but in a down-stroke mode. Christenson et al. (52) criticized this work by stating that molecules deposited in this fashion have to turn over on the substrate causing dangling polymer which might enhance the attraction by some other mechanism such as polymer bridging. This argument seems to be validated because the hydrophobic attraction

extended only upto ~30 nm when forces were measured between monolayers deposited in the up-stroke mode.

Another intriguing measurement is that reported by Wood and Sharma (53), who prepared a monolayer of Octadecyltriethoxy (OTE) silane on mica. The OTE was first polymerized by spreading it in the form of a L-B monolayer at the air-water interface, then deposited onto a plasma-activated mica and subsequently annealed at 120^{o}C. The surfaces were extremely hydrophobic as indicated by the fact that θ_a and θ_r were 111^{o} and 91^{o} respectively. Nevertheless, no long-range hydrophobic forces were observed. To explain their results, the authors obtained AFM images of OTE monolayers and observed that the layers were extremely homogenous and fully covered the mica surfaces, which is not the case with other L-B deposited monolayers. It was suggested that in the latter case, there are usually pinhole size (~45 nm) defects, which may expose the bare mica surface to the solution. Wood and Sharma explained their observations on the basis of a theory originally proposed by Miklavic *et al*. (54). The latter showed theoretically that if a hydrophobic mica surface is assumed to consist of a lattice, where hydrophobic patches co-exist with bare patches, the interaction forces between two such surfaces is a long-range attraction. It was argued that the L-B films of DDOA or other surfactants indeed consist of such an array of hydrophobic and bare mica patches whereas, OTE monolayers are relatively "defect" free. Wood and Sharma suggested, therefore, that domain or patch formation is necessary for appearance of a strong hydrophobic force.

(iv) Chemically modified surfaces

Rabinovich and Derjaguin (4) measured the forces between two methylated quartz fibers and observed an exponentially decaying attraction which could be expressed using a single-exponential function (Eq.[1]), with D_o=12 nm. Rabinovich and Yoon (56) used an AFM to measure the hydrophobic forces between silica surfaces silanated to different degrees (θ_a=88-115^{o}) using octadecyltrichlorosilane (OTS) and trimethylchlorosilane (TMCS). With surfaces exhibiting a θ_a of 115^{o}, the hydrophobic force was observed to be much larger than those with L-B monolayers of $DDOA^{+}$. Yoon *et al*. (37) compared the results of two different types of force measurements between OTS coated silica surfaces: one between two surfaces exhibiting the

same θ_a (symmetric measurements) and the other between surfaces exhibiting different θ_a (asymmetric measurements) hydrophobicities. For asymmetric measurements, the hydrophobicity of one surface was fixed at θ_a=109^o, while the other's was varied from 80^o to 109^o. The hydrophobic forces were expressed in terms of a power law. It was observed that the interaction parameter for the asymmetric interactions, K_{132}, where **1** and **2** represent surfaces of two different hydrophobicities interacting across a solvent **3**, could be related to the two symmetric measurements K_{131} and K_{232} by a simple geometric rule as follows:

$$K_{131} = \sqrt{K_{131} \times K_{232}} \tag{5}$$

Parker and Claesson (57) measured the forces between silanated silica surfaces using a different apparatus (bimorph), and observed hydrophobic force with a decay length of 5.6 nm. In another study, Parker *et al*. (58) exposed a mica surface to low temperature water plasma to make it more reactive to silanes. The surface was then allowed to react with silane vapor to yield a surface with θ_a=95^o and θ_r=70-75^o. Force measurements between two such surfaces indicated the presence of a hydrophobic force at separations<50 nm. Very recently, Ederth et al. (28) prepared gold surfaces by vacuum deposition onto smooth glass substrates, which were then placed in alkanethiol solutions to yield a robust monolayer. The largest θ_a obtained was 107^o and force measurements conducted with an SFA indicated the presence of an attractive force which caused the two surfaces to jump into contact at separations of 40 nm.

(v) Intrinsically Hydrophobic Surfaces

Several investigators conducted force measurements between naturally hydrophobic surfaces like teflon (33), polystyrene (26) and polypropylene (27) in water. All of these surfaces exhibited large values of θ_a (>100^o) and θ_r (>90^o). However, no long-range hydrophobic forces were observed with them. The attraction was at best medium-ranged, being discernable at separations less than 20-25 nm. The fact that the attraction between such extremely hydrophobic surfaces is not long-ranged is at odds with the idea that the force is a result of the hydrophobicity of the surface. Based on the results of the force measurements described in the foregoing

sections, various theories have been proposed for the origin of the hydrophobic force, as will be discussed in the following section

1.3b *Theories for the Hydrophobic Force*

(i) Forces due to Solvent Structure

Israelachvili and Pashley, who reported the first measurement of hydrophobic force (3) suggested that the hydrophobic force may be due to the changes in water structure near hydrophobic surfaces. The exponential force law (Eq.[1]) proposed by these authors, when extrapolated to molecular separations can predict accurately the free energy of interaction of two hydrophobic solutes in water. Similarly, in a much earlier publication, Laskowski and Kitchner (58), proposed that the instability of water films on hydrophobic substrates is "fundamentally due to a deficiency of hydrogen bonding in these films as compared to liquid water." Derjaguin and Churaev (59) proposed that the structural forces, which includes both the hydrophobic and hydration forces, may be a result of the overlap of structurally modified boundary layers of the liquid. It is well-known that near hydrophobic surfaces the water structure is different than in the bulk. This is because the inert hydrophobic surface offers no sites to the water molecule to form hydrogen bonds. Computer simulations have shown that at these interfaces, water molecules may undergo orientational reorganization to form an ice-like structure (60). Eriksson *et al*. (61) proposed that the hydrophobic force originates from the hydrogen-bond-propagated ordering effects in the water layer between two hydrophobic surfaces. This theory is based on the square gradient approximation of Marcelja and Radic (62), which was originally formulated to explain the hydration force between two hydrophilic surfaces.

Recent measurements have shown, however, that it is not uncommon for the hydrophobic force to extend up to 90 nm and in some exceptional cases even micron or submicron distances. It is not conceivable that water-structuring effects extend this far away from the surface. Simulations for the water structure (63) have shown that at distances approximately 0.7-1.0 nm away from the surface, bulk water structure is attained. Thus, based on solvent structuring effects, only a short-range hydrophobic force can be expected. Recall that some direct force

measurements revealed that the hydrophobic force may be better represented by a double exponential function (5). This suggests that there may actually be two components to the hydrophobic force: a strongly decaying short-range interaction and a slowly decaying long-range force. From force measurements between surfaces of varying hydrophobicities, Hato (50) concluded that only the short-ranged component shows a strong correlation with the hydrophobicity of the surface and is likely to be related to water structuring effects at the interface.

(ii) Theories based on an Electrostatic Mechanism

The idea that the hydrophobic force can be electrostatic in nature arose from observations that the hydrophobic force decreases with the addition of salt (3,5,36,40). Attard (64) suggested that the hydrophobic force is a result of the anomalous dielectric response of the aqueous fluid layer next to the hydrophobic surface. Using this approach, Attard obtained an attractive interaction which decayed at $\kappa^{-1}/2$, where κ^{-1} is the Debye length. This prediction was noted to be in agreement with a limited amount of experimental data. On the other hand, Podgornik (65) considered a model with specific ion adsorption and concluded that there would be a large correlation force when two such surfaces approach each other as a result of the lateral mobility of the adsorbed ions. Tsao *et al.* (41), while subscribing to Podgornik's mechanism for the hydrophobic force, suggested a different molecular origin. They proposed that these forces are a result of correlation of the large in-plane dipole moments associated with domains of adsorbed hydrocarbon molecules. Dipole moments may arise if surfactants adsorb on a substrate with tilted configurations (34). They may also arise because, in the vicinity of hydrophobic surfaces, water dipoles are known to be oriented in a parallel unidirectional manner (60,63,66).

Experimentally the domain theory was shown to be feasible by Tsao *et al*. (41) and Rabinovich and Yoon (67), who observed domains or clusters of surfactants molecules on silanated silica surfaces using an AFM. Flinn *et al*. (68) used an AFM to image OTS monolayers on silica and noted that, with increasing hydrophobicity (θ_a), domains do not grow in size. Rather, the packing density of hydrocarbon molecules inside the domains increases. These authors also measured the hydrophobic force between silanated silica surfaces of varying θ_a.

They concluded that the decay lengths of the measured hydrophobic forces vary with the domain size and distance between domains, while the strength is dependent on the packing density within the domains. Another electrostatic mechanism for the hydrophobic force is the correlation between lattice array of charges (54), which has been explained earlier in this chapter.

Nevertheless, the theory that the hydrophobic force may be electrostatic in nature is not universally accepted. This is partly because the exact dependence of the hydrophobic force on salt has not been established. Although many researchers have observed a decrease in the hydrophobic force upon addition of salt, this decrease is reflected more in the pre-exponential factor than in the decay length (40,51,52). Moreover, the decrease in decay length of the force if any, is not in agreement (39,49) with those predicted by the electrostatic mechanisms of Attard (64) and Podgornik (65). It has been argued that the decrease in hydrophobic force in the presence of salt maybe more due to a reduction in the hydrophobicity of the surface than in the hydrophobic force (36,68). This is because both SAMs and L-B layers are prone to being degraded and hydrophilized in the presence of salts.

Finally, it should be mentioned that there have also been reports in literature where the presence of electrolyte does not seem to have any effect on the hydrophobic forces. Meagher and Craig (26) observed this trend for hydrophobic forces between polypropylene surfaces. Wood and Sharma (53) reported the same behavior for the case of polymerized OTE layers on mica. On the other hand, Parker *et al.* (38) measured the forces between silica surfaces reacted with a fluorosilane and observed that at very high salt concentrations (1M KBr) the hydrophobic force increases slightly. The evidences presented above are difficult to reconcile with an electrostatic mechanism, which predicts that presence of electrolyte should reduce the magnitude of any force.

(iv) Cavitation

It is well known that the liquid film between two very hydrophobic surfaces is in a metastable state (69). Yaminsky *et al.* (70) proved theoretically that if the contact angle of a hydrophobic surface exceeds 90^{o}, the formation of a water-vapor cavity becomes

thermodynamically favored at small separations. Cavitation has been observed experimentally in many different systems (34,38,71). The size and shape of the cavities has also been shown to be consistent with the predictions of the Laplace Equation (71). Thus, the above evidences suggest that capillary forces associated with bridging capillaries may be one explanation for the hydrophobic force. Yaminsky and Ninham (72) suggested that even if the contact angle of the hydrophobic surface is less than 90^o, there is a possibility of an additional attractive force. This phenomenon is called *subcritical cavitation* and may be attributed to the enhanced thermal fluctuations of the intermolecular voids in the gap between two such surfaces. Nevertheless, as suggested by Yoon and Ravishankar (73), the magnitude of the forces predicted by this theory is of the order 1-2 times the vdW forces, which is too small to account for most of the experimental observations.

An interesting observation regarding the phenomenon of cavitation was made by Parker *et al*. (38) who conducted force measurements between fluorosilane treated glass surfaces (θ_a~110^o, θ_r~90^o). Large attractive hydrophobic force were observed extending upto ~250 nm. Further, steplike features were observed in the force curves during the approach cycle, which was attributed to the formation of cavities before contact. This observation is unique because all other experiments showed that cavitation may occur only during or after contact (34,71). Parker *et al*. attributed the long–range attraction to the bridging of submicroscopic cavities or bubbles between the surfaces and presented a theoretical model to fit the force data. This theory may also be supported by the observations that the presence of dissolved gas seems to enhance the hydrophobic attraction. Rabinovich and Yoon (67) measured the forces between a silanated silica plate and glass sphere in argon-saturated water and noted that the hydrophobic force was significantly higher in this case than in water saturated with air. This was attributed to the fact that argon is more soluble in water than air. Further, Meagher and Craig (26) observed that removal of dissolved gas reduces the range of hydrophobic interaction between two polypropylene surfaces. Nevertheless, the fact that long-range hydrophobic forces are absent in some cases between surfaces which exhibit contact angles much larger than 90^o (26,27,33,53) has raised serious objections to this theory.

(v) Others Theories

Ruckenstein and Churaev (74) suggested that the hydrophobic force may be a result of hydrodynamic correlations between fluctuations of the highly unstable water layer in the vicinity. These authors derived an attractive force varying with separation in the form of a power law with an exponent of –3, which is close to the value of –2 to –2.3 proposed in literature (5,36,37,71). Another theory proposed by Yaminsky *et al*. (75) relates the hydrophobic force in the case of SAMs to increased surfactant adsorption at a surface as the intersurface separation is decreased. Note, however, that this theory may not be applicable for the case of hydrophobic forces observed between LB deposited monolayers and silanated silica surfaces. Yaminsky and Christenson (76) suggested a modification of the above theory by noting that if the hydrophobic groups are laterally mobile on the surface, a local difference in the surface excess may be created leading to an attractive force. The absence of such groups on naturally hydrophobic surfaces like teflon, polystyrene and the annealed polymerized layers of OTE may explain why no long-range attraction is observed in these cases.

1.4 The Hydration Force

Hydration forces may be broadly classified as *primary* and *secondary* depending on their origin. The former is observed between surfaces in pure water, i.e. surfaces, which are naturally hydrated in water in the absence of any solutes. Examples of such surfaces include silica and lipid bilayers. The secondary hydration force, on the other hand, is observed between some surfaces only in the presence of hydrated cations. No hydration force is observed between such surfaces in pure water. To this category belong surfaces like mica and rutile. In the following sections, we shall look at experimental evidences and proposed theories of origin for both the primary and secondary hydration forces.

1.4a *Primary Hydration Force*

1.4a.1 Experimental Evidence

(I) *Evidence from Coagulation Studies of silica sols*: Allen and Matijevic (77) studied the stability of colloidal silica sols in solutions of NaCl, LiCl, KCl, CsCl, NaBr, NaI $CaCl_2$ and $Ca(NO)_2$ at various pHs. The sols were observed to be exceptionally stable towards electrolyte. At low pH values, none of the salts used were effective in destabilizing the suspensions regardless of their concentrations. This is surprising because close to pH 2, the silica surfaces are electrically neutral and silica particles are expected to coagulate due to attractive van der Waals forces. Further, at higher pH values, where coagulation did occur, the concentrations required were much larger than those predicted by the Schulze-Hardy rule.

Allen and Matijevic also noted that the critical coagulation concentration (ccc) for each cation decreases linearly with increasing pH in the pH range of 6-10. Further, the ccc of the cations was found to follow the order $Li^+ > Na^+ > K^+ > Cs^+$, which is the reverse of the Hoffmeister series. Interestingly, this trend is exactly the opposite of the ability of alkali metal ions to exchange with the proton of the surface silanol groups. Earlier results with titration of silica in the presence of cations had shown that the ability to exchange with the proton of SiOH decreases in the order $Cs^+ > K^+ > Na^+ > Li^+$. Thus, the cation with the greatest propensity for ion exchange is observed to have the lowest ccc and vice versa. Therefore, the authors concluded that the destabilization of silica sols in the presence of electrolyte proceeds by ion exchange. Watillon and Gerard (78) had suggested earlier that the exceptional stability of silica sols may be attributed to steric repulsion caused by the presence of a monolayer of water molecules adsorbed on silica. The exact mechanism of this repulsion will be discussed in detail in Section 1.2a.2. Suffice to say here that these water molecules are hydrogen bonded to the silanol groups on the silica surface. When a cation exchanges with the proton of the silanol, the silica surface loses one site for H-bonding with water. Thus, ion-exchange progressively depletes the silica surface of the stabilizing layer of water molecules. It was suggested that when a critical number of protons of SiOH have been replaced by the cation, the silica sol is destabilized.

The results of Allen and Matijevic were obtained in the pH range 6-10 and the observed trend in ccc values is valid only upto pH<10. Depasse and Watillon (79) conducted coagulation experiments with silica sols at pH>11 and found that at highly alkaline pH, only Li^+ and Na^+ were capable of coagulating silica, whereas K^+, Rb^+ and Cs^+ were not. The explanation given for

this was that at such pH the silica surface is largely covered by basic SiO^- groups. This is unlike the situation in the lower pH, where the silica surface is covered with undissociated silanol groups. At higher pH, it is possible that only Li^+ and Na^+ can react with the basic SiO^-. This is because among all the alkali metal ions, only these two show acidic characters.

Yoon and Yotsumoto (80) conducted turbidity measurements with precipitated silica in aqueous solutions of NaCl. They estimated the magnitude of the hydration energy using an extended DLVO theory, where the hydration energy was expressed in the form of Eq.[3]. From their experiments, the authors obtained the following parameters for the hydration force in 0.2M NaCl solution at pH 2.0: C_1=8.3 mJ/m^2, C_2=0.44 mJ/m^2, D_1=0.92 nm and D_2=3.0 nm. When the concentration of NaCl was increased to 5.4 M, it was observed that the values of C_2, D_1 and D_2 remained practically the same while, C_1 decreased drastically to 1.08 mJ/m^2. This is again consistent with the observations of Allen and Matijevic, who showed that increase in electrolyte concentration may promote destabilization of silica suspensions. An increase in electrolyte concentration should increase the ion exchange with the surface silanol, thereby depleting the surface of the proton, which promotes water structure around silica.

(II) *Direct Measurement of Primary Hydration Forces*: In the last section, we examined indirect experimental evidences for the primary hydration force, as obtained from coagulation experiments. The first direct measurement of the primary hydration force was by LeNevue et al. (81), who devised a method for measuring the forces between planar phospholipid layers. The authors measured the osmotic force between hydrated phosphatidyl choline bilayers in water and observed monotonically decaying hydration repulsive forces at bilayer separations of less than 3 nm. Further, it was noted that the hydration repulsion decays exponentially with distance and had a decay length of 0.19 nm. Later Persson and Bergstahl (82) showed the existence of monotonic hydration repulsion between lecithin bilayers in ethylene glycol, which is a H-bonding solvent.

Rabinovich and Derjaguin (7) measured the forces between two crossed glass fibers in KCl solutions and showed the existence of hydration forces which could be represented using Eq.[2] with D_o=0.85 nm. It was observed that the hydration force decreases with increasing

electrolyte concentration. Peschel *et al*. (83) used a different technique to measure hydration force between polished silica plates in aqueous solutions of LiCl, NaCl and KCl. The magnitude of the hydration force was found to decrease in the order of KCl>NaCl>LiCl. Note that this trend is exactly the opposite of the ability of the cations to exchange with the surface silanol group. This result is surprising since one would expect that if, for example, Li^+ is the least adsorbed cation on the silica surface, it should destroy the hydration force the least.

Similar results have also been obtained by Chapel (84), who used the SFA to conduct force measurements between two cylindrical silica sheets immersed in a series of alkali salt solutions. The magnitude of the hydration repulsion was found to decrease in the order $Cs^+>K^+>Na^+>Li^+$. Chapel also used a site-binding model to fit his force data to the DLVO theory and to calculate the amount of cation adsorbed on the silica surface. It was found that the amount of cations adsorbed on silica follows the order $Cs^+>K^+>Na^+>Li^+$. Peschel *et al*. and Chapel suggested that the trend in hydration repulsion should be explained in terms of a model, which assigns the magnitude of the repulsion to the difference in chemical potential between the cation in the surface layer and the bulk. Since the hydration repulsion is the smallest for Li^+, the difference in chemical potential for the case of Li^+ should be the least. This indicates that Li^+ should be the least adsorbed on the surface. Thus, this theory explains both the trend in hydration force and the ability of the cations to exchange.

Horn *et al*. (85) studied the surface forces and viscosity of water between silica sheets. Since the method of preparation of the silica sheets involved melting the silica, the surfaces exhibited a low degree of hydroxalation as evidenced by the high advancing water contact angle of ~45^o. Nevertheless, the force data showed evidence for a short-range repulsion at distances <2 nm. The authors ascribed this to the presence of a modified water structure at the silica interface. However, viscosity measurements indicated no difference between bulk water and surface water layers. Grabbe *et al*. (86) conducted force measurements after preparing the silica with one of three surface treatments: (i) flaming (ii) exposure to steam for 150 h and (iii) exposure to ammonia. The hydration repulsion was observed to be unaffected by any surface treatment. The hydration force in this work was also expressed in the form of Eq. [2] with the following parameters: C_1=140 mJ/m^2, C_2=5.4 mJ/m^2, D_1=0.057 nm and D_2=0.48 nm.

Ducker *et al*. (11) were the first to use the Atomic Force Microscope for direct measurement of surface forces. They measured the forces between a silica plate and a glass sphere in aqueous electrolyte solutions. The authors reported that at very short distances (<5 nm), the force data deviates from the DLVO theory possibly due to the presence of the hydration force. Finally, Vigil *et al*. (87) conducted various experiments to measure the adhesion, friction and colloidal forces between silica surfaces using the SFA. Based on their results, they concluded an entirely different origin for the "hydration force". They suggested that the unusual behavior of colloidal silica is not due to hydration effects, but rather due to the presence of a thick *gel-like* layer of protruding silanol and silicic acid groups that grow on surfaces in the presence of water. This mechanism is detailed in the section 1.2a.3.

1.4a.2 Theories for the Primary Hydration force

(I) *Water Structure Theory:* As noted in the last two sections, there is no dearth of experimental evidences in literature for the existence of primary hydration force. Many researchers (7,77,78,83,84) have suggested that the origin of the monotonically repulsive hydration force between silica surfaces may be related to the structuring of water molecules at the silica-water interface. It is well known that water can form strong H-bonds with the silanol groups. Klier and Zettlemoyer (88) have shown that the water molecule sits "oxygen down" on the SiOH groups. This would imply that in the formation of a H-bond between water and SiOH, the water molecule acts as a base and the SiOH as the acid. The energy of interaction of the water molecule with the silanol group can be determined by microcalorimetry. This technique (89) yields a value of -25 kJ/mol for the formation of the water silanol bond. Theoretical models, on the other hand, predict the binding energy to be ~-32 kJ/mol (90). Ugliengo *et al*. (91) calculated the binding energy of water to silanol considering two modes of interactions: (I) water as a proton donor and (II) water as a proton acceptor. It was concluded that the configuration II was the most stable thermodynamically, which is in agreement with the observations of Klier and Zettlemoyer. It should be mentioned here that the adsorbed water molecule may also form H-bonds with two adjacent silanol groups. In such cases, water acts as both a proton donor and acceptor. Obviously, the binding energy in this configuration is much higher ~-60 to -90 kJ/mol (92).

Iller (93) has suggested that a fully hydroxalated silica surface is almost entirely covered with adsorbed water molecules. Dalton and Iler (94) concluded from viscosity measurements that there is definitely a monolayer of water molecules immobilized at the SiOH surface by hydrogen bonding. On the other hand, Derjaguin (95) suggested that next to the silica surface there might be a layer of structured water upto 900 A^o thick. Though it is doubtful whether the structure of water extends this far from a surface, there is evidence from molecular dynamics simulations (96) that at least the first few layers of water molecules are oriented by polar surfaces. Assuming that the presence of hydrophilic surfaces imposes a structure on the water molecules in the vicinity, Marcelja and Radic (62) proposed an elegant theory to explain the nature of the hydration force. The free energy of the system was expressed in terms of an order parameter, which represents the water structure. Minimization of this free energy resulted in a water structure that decays from each surface, giving rise to an exponentially decaying repulsive force between hydrophilic surfaces. However, this theory does not satisfactorily explain various experimental observations. The decay length of the hydration force predicted by this theory is of the order of molecular separations. Experimental measurements have often yielded decay lengths larger than this by an order of magnitude. Moreover, the hydration force seems to be better represented by a double exponential function rather than a single exponential one.

Attard and Batchelor (97) proposed a different mechanism for the hydration force based on the orientation of water molecules near polar surfaces. It was suggested that due to the strong orientation of water molecules near the polar surface, there are fewer configurations available to maintain the bulk water structure. This represents lost entropy, which leads to a repulsive force. Besseling (98) further extended this model by taking into account the changes in both orientation and local density of fluid molecules at planar surfaces. It was observed that if the main effect of the surface is to change the local orientation of water molecules, the result is a repulsive force similar to the hydration force. However, if the surface alters the local density without changing the orientation, the result is an attractive force, similar to the hydrophobic force.

Israelachvilli and Wennerstrom (99) have argued, on the other hand, that any force arising from structuring of water molecules can only be attractive or oscillatory. The fact that

forces due to water structure may be oscillatory has been experimentally confirmed (14,15). Oscillatory forces are discussed in detail in connection with secondary hydration forces later in this chapter. Attractive forces arising out of water structure have indeed been measured for hydrophobic surfaces. Israelachvilli and Wennerstrom contend that this should be true for polar surfaces also. The authors presented a conceptual model to prove that the perpendicular orientation of water dipoles on opposing polar surfaces can only lead to an attraction not repulsion. It was suggested that repulsive hydration forces have an entirely different origin depending on the nature of the interacting surfaces rather than the structure of the intervening solvent. For example, the "hydration forces" between lipid bilayers may be result of *undulation, peristaltic* and *protrusion* forces (19,100). These forces arise because the bilayer membranes are not rigid and can have significant thermal undulations. In the presence of an opposing surface, these motions are restricted and this might give rise to a repulsive force. On the other hand, the hydration forces between silica surfaces may be due to the presence of silicic acid hairs as suggested by Vigil *et al*. (87).

(II) *Silica Hair/Silica Gel Theory*: The presence of a porous gel-like layer on silica was proposed by Lyklema (101) to explain the high surface charge and low potentials of the silica surface. Theoretical calculations to account for the observed charging characteristics of oxides have indicated that the gel layer maybe ~2-6 nm thick (102). Experimental evidence for the existence of a gel layer was presented by Vigil *et al*. (87), who used the SFA to study colloidal interactions between cylindrical silica sheets in water. They observed that when compared to the contact position (Separation distance=0 nm) in dry air, the contact in water or humid air is shifted out by 2-4 nm. This was attributed to the growth of a 1-2 nm thick silica gel layer of silanol and silicic acid groups (hairs) at each surface due to adsorption of water on silica. The swelling of the surface may be further enhanced by the electrostatic repulsion between negatively charged SiO^- groups on both the hairs and the surface, so that the resulting gel-layer on silica resembles a polymer brush. Consequently, when two gel layers overlap at smaller separations, there may be an additional monotonic steric repulsion which .explains the observed "hydration" repulsion between silica surfaces. Alternatively, the presence of charged hairs might shift the location of plane of charge of the surface slightly outward. Even if this outward shift is only 0.5 nm, the net interactions may become more repulsive at separations distances as large as

4 nm. The reduction of the hydration repulsion in aqueous electrolyte solutions can also be explained by the silica hair theory. In the presence of cations, the polymeric silica hairs may collapse due to screening of the electrical repulsion between the charged hairs. This mechanism is very similar to the collapse of polymers in bad solvents. The net effect of this would be a reduction in the range of both the steric repulsion and the electrical repulsion due to the shift in the plane of charge.

(III) *Theories Based on Modification of the DLVO Theory:* Various modifications of the double layer have been proposed to explain the origin of the hydration force, all of which result in an extra repulsive force at short separations. Some of these theories propose that hydration force arises because the DLVO theory does not take into account the finite size of the ions or specific interactions of ions with surfaces. These will be discussed in the section on secondary hydration forces since the primary hydration forces are observed in pure water even when the concentration of ions is extremely low.

Gruen and Marcelja (103,104) proposed an elaborate theory to explicitly take into account the microscopic structure of the solvent. The result was a generalized expression that was seen to predict a short-range hydration repulsion in addition to the classical double layer repulsion. Schiby and Ruckenstein (105) developed a mathematical model assuming that the surface polarizes the first layer of water molecules which in turn polarizes the next layer and so on. In effect, they assumed a polarization function varying with distance from the surface. Calculations showed that when the polarized water layers of two such surfaces overlap, a hydration force results which has a decay length of 2.4 A^o. Though this might explain the hydration force observed between lipid bilayers, the decay length obtained here is too small to account for the results obtained with silica. Henderson and Lozada-Cassau (106) suggested that since the water molecules at the surface are strongly oriented, there should be a region of smaller dielectric constant at the solvent substrate interface when compared to the bulk. The authors incorporated this into the DLVO theory and observed a repulsive force at small separation distances. Nevertheless, none of the proposed modifications to the DLVO theory have found universal acceptance mainly because no single theory can explain all the experimental observations.

1.4b *Secondary Hydration Force*

1.4b.1 Experimental Evidence

(I) *Evidence from coagulation of rutile (TiO_2) suspensions*: Yoon and Yotsumoto (13) conducted turbidity measurements with rutile suspensions in aqueous solutions of NaCl. It was observed that at low NaCl concentrations ($<2x10^{-2}$M), the stability behavior of rutile can be predicted based on the classical DLVO theory. Thus, rutile does not show any evidence for the primary hydration force. However, at concentrations$>2x10^{-2}$M, the suspensions were noted to exhibit stability greater than that predicted by the DLVO theory. At concentrations>1 M, the suspension was redispersed even at its IEP. This additional stability was attributed to the secondary hydration force resulting from the adsorption of hydrated cations on the rutile surface. The authors also used the extended DLVO theory to calculate the hydration energy, which was represented by Eq.[3]. It was noted that the parameters C_1, C_2, D_1 and D_2 are of the same order as those for silica.

(II) *Direct Measurement of the Secondary Hydration Force*: Secondary hydration forces were first measured by Pashley (107) between mica surfaces in aqueous solutions of the alkali metal ions Li^+, Na^+, K^+ and Cs^+. Subsequently, Pashley and Israelachvili (108) also noted the existence of these forces between mica surfaces in solutions of alkaline earth cations Mg^{2+}, Ca^{2+}, Sr^{2+} and Ba^{2+}. With all these cations, at low concentrations, the experimental force data could be fitted to the DLVO theory perfectly and there was no evidence of the hydration repulsion. Further, it was noted that for each cation, there is a critical concentration, known as the critical hydration concentration (CHC) beyond which hydration repulsion is observed. The strength of the secondary hydration force in the presence of the alkali metal ions was found to decrease in the order $Li^+ \sim Na^+ > K^+ > Cs^+$. Recall that this is exactly the opposite of the order observed for the primary hydration force with silica. In the presence of divalent cations, the hydration force was noted to be stronger than that for monovalent cations. The D_2 in the case of the latter varies from ~0.3 nm for Cs^+ to ~0.9 nm for Na^+. With divalent cations the D_2 is larger ~1.8-2.0 nm.

To explain why hydration repulsion is observed only at concentrations>CHC, Pashley calculated the adsorption density of cations on silica using the ion-exchange model. However, no sharp increase in adsorption was noted at CHC. Therefore, it cannot be suggested that the appearance of the hydration force at CHC is related to a sudden increase in adsorption of hydrated cations. On the other hand, it was suggested that at concentrations below CHC, hydronium ions may displace the adsorbed cations just before the two surfaces come into molecular contact. It is well known that the presence of adsorbed hydronium ions on mica does not give rise to hydration repulsion. However, when the bulk concentration of the cations is larger than the CHC, it becomes thermodynamically unfavorable for the above displacement to occur. The hydrated cations now remain adsorbed on mica giving rise to a repulsive hydration force. Further, Pashley suggested that it is the dehydration of the adsorbed cation that results in hydration repulsion. Since Li^+ is more strongly hydrated than Cs^+, the hydration force decreases with decreasing strength of hydration of the cation. Divalent cations are more strongly hydrated than monovalent ions, hence the hydration force is stronger in the case of the former.

Finally, one important difference between the primary and secondary hydration forces was pointed out by Israelachvili and Pashley, who also conducted (14) detailed and accurate measurements of secondary hydration force between mica surfaces at separations less than 1.5 nm. Forces were measured in 10^{-3}M KCl solution and it was observed that although the secondary hydration force is overall repulsive, it is not monotonic at separations<1.5 nm. There is an oscillatory component superimposed on the monotonic repulsion and the mean periodicity of the oscillations is ~0.25 nm, roughly the diameter of a water molecule. Similar oscillatory forces had been measured earlier in other non-polar and polar organic solvents (15,109). In each case the oscillation was observed to be roughly equal to the diameter of the particular solvent molecule. However, in the case of the primary hydration force between silica surfaces or lipid bilayers, the oscillatory component has never been observed. This was explained by suggesting that only at molecularly smooth surfaces like mica, solvent molecules tend to stack in ordered layers. Each oscillation corresponds to the squeezing out of one layer of the solvent. It was also proposed that even a slight roughness can destroy this ordered layering and smear out the oscillations. This is perhaps what happens at the silica surface. On the other hand, lipid membranes are fluid-like and highly mobile. In this case, the thermal fluctuations and undulations of these membranes may smear out the oscillatory character of the hydration force.

1.4b.2 *Theories for the Secondary Hydration Force*

As seen earlier, the secondary hydration force has two components, the oscillatory and the repulsive. It is evident from experimental results that the oscillatory component is due to the ordered layering of water molecules. Pashley (107) has suggested that the monotonic component arises due to the dehydration of the adsorbed cations, which agrees well with the fact that the hydration force is stronger for the case of the more strongly hydrated cations.

Other mechanisms have also been suggested to explain the origin of the monotonic repulsion in the presence of ions. Almost all of these theories are based on certain modifications to the DLVO theory. One of the assumptions in the DLVO theory is that the counterions are treated as point charges. Ruckenstein and Schiby (110) suggested a modification to the Boltzmann distribution to account for the volume exclusion of the hydrated cations. Using this approach a larger double layer repulsion was observed that at small separation distances, which may explain the appearance of the repulsive hydration force. Spitzer (111) proposed that if two charged surfaces approach each other in such a way that the co-ions are completely expelled from the double layer, then a large repulsive force arises. The magnitude of this repulsion was seen to be in agreement with the experimentally measured repulsive pressure between montmorillonite surfaces. In a recent paper, Ninham and Yaminsky (112) suggested that the usual decomposition of colloidal forces into van der Waals and double layer forces is invalid and that these are, in fact, coupled. The authors also stressed the need to consider the dispersion forces acting on ions to provide a more complete theory.

1.5 Research Objectives

The overall objective of this investigation was to examine how hydration and hydrophobic forces are affected in the presence of different reagents. An attempt has also be been made to delineate the mechanisms by which these solutes may affect the two non-DLVO forces. It is expected that the results obtained will demonstrate how these two forces can be manipulated

using suitable reagents and, at the same time, shed some light on the origin of the hydration and hydrophobic forces. The specific goals of this research include:

a) to conduct direct force measurements for the hydrophobic forces in dioctylammonium (DOAHCl) chloride solutions in the presence and absence of octanol.

b) to measure the primary hydration forces between silica surfaces in the presence of methanol, ethanol, trifluoroethanol (TFE) and pyridine. Each of these solutes has a different propensity to form hydrogen bonds with the silanol group.

c) to study the effect of hydrolizable cations on the hydration and hydrophobic forces. In order to do this, force measurements were conducted with both hydrophilic and hydrophobized silica surfaces in the presence of these cations at different pHs.

d) to discuss the mechanisms of adsorption of hydrolizable cations on both hydrophilic and hydrophobized silica in view of the results obtained in (c).

e) to measure the hydrophobic forces between silica surfaces hydrophobized by anionic surfactant (sodium oleate).

1.6 Report Organization

The results obtained in the present work have been reported in Chapters 2 to 5. Each chapter comprises of an introduction, experimental, results, discussion and conclusion sections and may be considered as an article for publication. In Chapter 2, the results of surface force measurements conducted with the secondary amine (DOAHCl) in the presence and absence of octanol are reported. The surface tension of DOAHCl solutions was first measured to determine its surface activity and the critical micelle concentration (CMC). Advancing (θ_a) and receding (θ_r) water contact angles were measured at varying DOAHCl and octanol concentrations. Force measurements were conducted in solutions containing varying concentrations of DOAHCl and octanol. The decay lengths (D_2) of the measured hydrophobic forces were plotted as a function of the advancing contact angle. The thickness of the adsorbed layer was used to estimate the

hydrocarbon chain density in the monolayers. The results obtained show a clear correlation between hydrocarbon density, θ_a and D_2.

In Chapter 3, the effect of methanol, ethanol, trifluoroethanol (TFE) and pyridine on the primary hydration forces between silica surfaces was studied. The results obtained are evaluated in terms of the propensity of each of these solutes to displace the water molecules H-bonded to the silanol groups of silica, which may explain the observed changes in hydration force.

In Chapter 4, the results of the force measurements conducted with activated silica surfaces in sodium oleate solutions are reported. Two hydrolizable cations (Mg^{2+} and Ca^{2+}) were used as activators. The measurements were conducted in the presence of these activators to determine the changes in the primary hydration forces of silica that may be modified by them. The results were conducted by changing the pH of the electrolyte solution, and the results were compared with the species distribution diagrams for the two activators. This will give information on the nature of the activating species. Force measurements were also conducted in the presence of sodium oleate and Mg^{2+} (or Ca^{2+}) ions to detect the hydrophobic forces created by the oleate adsorption. Based on the results obtained, possible mechanisms have been suggested for the adsorption of the hydrolizable cations and the anionic surfactant on silica.

In Chapter 5, the results of the hydrophobic force measurements conducted with silanated silica surface in the presence of Cu^{2+} ions are reported. The results obtained in this chapter are discussed in view of the mechanism proposed in Chapter 4.

Finally, Summary and Conclusions and the Future work are given in Chapters 6 and 7 respectively.

1.7 References

1. Derjaguin, B. V., and Landau, L. *USSR Acta Physicochim*. **14,** 633 (1941).
2. Verwey, E. J., and Overbeek, J. Th. G. *Theory of the Stability of Lyophobic Colloids* Elsiever, New York, 1947.
3. Israelachvili, J., and Pashley, R. M. *Nature* **300,** 341 (1982).
4. Rabinovich, Ya. I. and Derjaguin, B. V. *Colloids and Surfaces* **30,** 243 (1988).
5. Claesson, Per M. and Christenson, H. K. *J. Phys. Chem.* **1988,** 92, 1650
6. LeNeveu, D. M., Rand, R. P., and Parsegian, V. A. *Nature* **259,** 601 (1976).
7. Rabinovich, Ya. I., Derjaguin, B. V. and Churaev, N. V. *Adv. Colloid Interface Sci.* **16,** 63 (1982).
8. Peschel, G., Belouschek, P., Muller, M. M., Muller, R. M., and Konig, R. *Colloid Polymer Sci*. **260,** 444 (1982).
9. Horn, R. G., Smith, D. T., and Haller, W. *Chem. Phys. Lett.* **162,** 404 (1989).
10. Grabbe, A. and Horn, R. G. *J. Colloid Interface Sci*. **157,** 375 (1993).
11. Ducker, W. A., Senden, T. J., and Pashley. R. M. *Nature* **353,** 239 (1993).
12. Pashley, R. M. *J. Colloid Interface Sci*. **83,** 531 (1981).
13. Yotsumoto, H. and Yoon, R. H. *J. Colloid Interface Sci.* **157,** 426 (1993).
14. Israelachvili, J. N., and Pashley, R. M. *Nature* **306,** 249 (1983).
15. Horn, R. G. and Israelachvili, J. N. *J. Chem. Phys.* **75,** 1400-1411 (1981).
16. Pashley, R. M. and Ninham, B. W. *J. Phys. Chem.* **91,** 2902 (1987)
17. Richetti, P. and Kekicheff, P. *Phys. Rev. Lett.* **68,** 1951 (1992)
18. Kjellander, R. and Marcelja, S. *J. Phys.* (*Paris*) **49,** 1009 (1988)
19. Helfrich, W. and Naturforsch, C. *Biochem. Biophys. Biol. Virol.* **281,** 693 (1973)
20. Israelachvili, J. N. and Adams, G. E. *J. Chem. Soc., Faraday Trans. 1* **74,** 975 (1978)
21. Tabor, D. and Winterton, R. H. S. *Proc. R. Soc. London,* A **312,** 435 (1969).
22. Steinberg, S., Ducker, G. V., Hyukjin, C. F., Tseng, M. Z., Clarke, D. R., and Israelachvili, J. N., *Science* **260,** 656 (1993).
23. Horn, R.G., Clarke, D. R. and Clarkson, M. T. *J. Mater. Res.* **3(3),** 413 (1988).
24. Parker, J. L. *Langmuir* **8,** 551 (1992).
25. Ducker, W. A., Senden, T. J. and Pashley, R. M. *Nature (London)*, **353,** 239 (1991).

26. Meagher, L. and Craig, V. S. J. *Langmuir* **10,** 2736 (1994).
27. Karaman, M. E., Meagher, L. and Pashley, R. M. *Langmuir* **9,** 1220 (1993).
28. Ederth, T.E., Claesson, P. and Liedberg, B. *Langmuir* **14,** 4782 (1998)
29. Biggs, S., Mulvaney, P., Zukoski, C. F. and Grieser, F. *J. Am. Chem. Soc.* **116,** 9150 (1994).
30. Atkins, D. T. and Pashley, R. M. *Langmuir* **9,** 2232 (1993).
31. Yoon, R. H. and Pazhianur, R *Colloids Surf.* Accepted fro publication
32. Biggs, S. *Langmuir* **11,** 156 (1995).
33. Tsao, Y. H., Evans, D. F. and Wennerstrom, H. *Science* **262,** 547 (1993).
34. Pashley, R. M., McGuiggan, P. M., Ninham, B. W. and Evans, D. F. *Science* **229,** 1088 (1985).
35. Craig, V. S. J., Ninham, B. W. and Pashley, R. M. *Langmuir* **14,** 3326 (1998).
36. Claesson, P. M., Blom, C. E., Herder, P. C. and Ninham, B. W. *J. Coll. Interface Sci.* **114,** 234 (1986)
37. Yoon, R. H, Flinn, D. F. and Rabinovich, Ya. I., *J. Coll. Interface Sci.* **185,** 363 (1997)
38. Parker, J. L., Claesson, P. M. and Attard, P. *J. Phys. Chem.* **98,** 8468 (1994).
39. Christenson, H. K., Fang, J., Ninham, B. W. and Parker, J. L. *J. Phys. Chem.* **94,** 8004 (1990).
40. Christenson, H. K., Claesson, P. M., Berg, J. and Herder, P. C. *J. Phys. Chem.* **93,** 472 (1989).
41. Tsao, Y-H., Yang, S. X, and Evans, D. F. *Langmuir*, **7,** 3154 (1991).
42. Pashley, R. M., McGuiggan, P. M., Horn, R .G. and Ninham, B. W. *J. Coll. Interface*
43. Kekicheff, P., Christenson, H. K. and Ninham, B. W. *Colloids Surf.* **40,** 31 (1989).
44. Herder, P. C. *J. Coll. Interface Sci.* **134,** 346 (1989).
45. Parker, J. L., Yaminsky, V. V. and Claesson, P. M. *J Phys. Chem.* **97,** 7706 (1993).
46. Yoon, R.-H., and Ravishankar, S. A. *J.Coll. Interface Sci.* **166,** 215 (1994).
47. Rutland, M., Waltermo, A. and Claesson, P. *Langmuir* **8,** 176 (1992).
48. Rabinovich, Ya. I., Guzonas, D. A. and Yoon, R.-H. *Langmuir* **9,** 1168 (1993).
49. Claesson, P. M., Herder, P. C., Blom, C. E. and Ninham, B. W. *J. Coll. Interface Sci.*

118, 68 (1987).

50. Hato, M. *J. Phys. Chem.* **100,** 18530 (1996).
51. Kurihara, K. and Kunitake, T. *J. Phys. Chem.* **114,** 10927 (1992).
52. Christenson, H. K., Claesson, P. M. and Parker, J. L *J. Phys. Chem.* **96,** 6725 (1992).
53. Wood, J. and Sharma, R. *Langmuir* **11,** 4797 (1995).
54. Miklavic, S. J., Chan, D. Y. C., White, L. R. and Healy, T. W. *J. Phys. Chem.* **98,** 9022 (1994).
55. Rabinovich, Ya. I. and Yoon. R.-H. *Langmuir* **10,** 1903 (1994).
56. Parker, J. L. and Claesson, P. M. *Langmuir* **10,** 635 (1994).
57. Parker, J. L., Cho, D. L. and Claesson, P. M. *J. Phys. Chem.* **93,** 6121 (1989).
58. Laskowski, J. and Kitchner, J. A. *J. Coll. Interface Sci.* **29,** 670 (1969).
59. Derjaguin, B. V. and Churaev, N. V. *Colloids Surf.* **41,** 223 (1989).
60. Kjellander, R. and Marcelja, S. *Chem. Scr.* **25,** 73 (1985).
61. Eriksson, J. C., Ljunggren, S. and Claesson, P. M. *J. Chem. Soc. Faraday Trans. 2* **85,** 163 (1989).
62. Marcelja, S. and Radic, N. *Chem. Phys. Lett.* **42,** 129 (1976).
63. Lee, C. Y., McCommon, J. A. and Rossky, J. *J. Phys. Chem.* **80,** 4448 (1984).
64. Attard, P. *J. Phys. Chem.* **93,**6441 (1989).
65. Podgornik, R. *J. Chem. Phys.* **91,** 5840 (1989).
66. Scott, H. L. *Chem. Phys. Lett.* **109,** 570 (1984).
67. Rabinovich, Ya. I. and Yoon, R.-H. *Colloids Surf.* **93,** 263 (1994).
68. Eriksson, L. G. T., Claesson, P. M., Ohnishi, S. and Hato, M *Thin Solid Films* **300,** 240 (1997).
69. Yuschenko, V. S., Yaminsky, V.V and Schukin, E. D. *J. Colloid Interface Sci.* **96,** 307 (1983).
70. Yaminsky, V.V., Yuschenko, V. S., Amelina, E. A. and Schukin, E. D. *J. Colloid Interface Sci.* **96,** 301 (1983).
71. Christenson, H. K. and Claesson, P. M. *Science* **239,** 390 (1987)
72. Yaminsky, V. V. and Ninham, B. W. *Langmuir* **9,** 3618 (1993).
73. Yoon, R.-H. and Ravishankar, S. A. *J. Colloid Interface Sci.* **179,** 391 (1996).
74. Ruckenstein, E. and Churaev, N. V. *J.Colloid Interface Sci.***147,** 535 (1991).

75. Yaminsky, V. V., Ninham, B.W., Christenson, H. K. and Pashley, R. M. *Langmuir* **12,** 1936 (1996).
76. Christenson, H. K. and Yaminsky, V. V. *Colloids Surf.* **129-130,** 67 (1997).
77. Allen, L. H. and Matijevic, E. J. *Colloid and Interface Sci.* **31,** 287 (1969).
78. Watillon, A. and Gerard, PH. *Proc. Int. Congr. Surface Activ.* **4,** 1261 (1964).
79. Depasse, J. and Watillon, A. *J. Colloid Interface Sci.* **33,** 430 (1970).
80. Yoon, R.-H. and Yotsumoto, H. *J. Colloid Interface Sci.* **157,** 427 (1993).
81. LeNeveu, D. M., Rand, R. P., and Parsegian, V. A. *Nature* **259,** 601 (1976).
82. Persson, K. T. and Bergenstahl, B. A. *Biophys. J.* **47,** 743 (1985).
83. Peschel, G., Belouschek, P., Muller, M. M., Muller, R. M., and Konig, R. *Colloid Polymer Sci*. **260,** 444 (1982).
84. Chapel, J.*Langmuir*, **10**, 4237 (1994).
85. Horn, R. G., Smith, D. T., and Haller, W. *Chem. Phys. Lett.* **162,** 404 (1989).
86. Grabbe, A. and Horn, R. G. *J. Colloid Interface Sci.* **157,** 375 (1993).
87. Vigil, G., Xu, Z., Steinberg, S., and Israelachvili, J. N. *J. Colloid Interface Sci.* **165,** 367 (1994).
88. Klier, K. and Zettlemoyer, A. C. *J. Colloid Interface Sci.* **58,** 216 (1977).
89. Bolis. V, Cavengo. A., and Fubini, B. *Langmuir* **13,** 895 (1997).
90. Abintio
91. Ugliengo
92. Fubnini, , Bolis, Cavengo and Ugliengo, P. *J. Chem. Soc. Faraday Trans.* **88,** 277 (1992)
93. Iler, R. K. *The Surface Chemistry of Silica*
94. Dalton, R. L. and Iler, R. K. *J. Phys. Chem.* **60,** 955 (1956).
95. Derjaguin, B. V. *Disc. Faraday Soc.* **42,** 109 (1966).
96. Berkowitz, M. L. and Raghavan, K. *Langmuir* **7,** 1042(1991)
97. Attard, P. and Batchelor, M. T. *Chem. Phys. Lett.* **149,** 206 (1988).
98. Besseling, N. M. *Langmuir* **13,** 2113 (1997).
99. Israelachvili, J. N. and Wennersrom, H. *Nature* **379,** 219 (1996).
100. Israelachvili, J. N. and Wennersrom, H. *J. Phys. Chem.* **96,** 520 (1992).
101. Lyklema, J. *J. Electroanal. Chem.* **18,** 341 (1968).

102. Peram, J. W., Hunter, R. J. and Wright, H. J. L. *Chem. Phys. Lett.* **23,** 265 (1973).
103. Gruen, D. W. R. and Marcelja,S. *J. Chem. So. Faraday Trans. 2* **79,** 211 (1983).
104. Gruen, D. W. R. and Marcelja,S. *J. Chem. So. Faraday Trans. 2* **79,** 225 (1983).
105. Schiby, D. and Ruckenstein, E. *Chem. Phys. Lett.* **95,** 435 (1983).
106. Henderson, D. and Lozada-Cassau, M. *J. Colloid Interface Sci.* **114,** 180 (1986).
107. Pashley, R. M. *J. Colloid Interface Sci.* **83,** 531 (1981).
108. Pashley, R. M. and Israelachvili, J. N. *J. Colloid Interface Sci.* **97,** 446 (1984).
109. Christenson, H. K. *J. Phys. Chem.* **90,** 4 (1986).
110. Ruckenstein, E. and Schiby, D. *Langmuir* **1,** 612 (1985).
111. Spitzer, J. J.*Nature*
112. Ninham, B. W., and Yaminsky, V. *Langmuir* **13,** 2097 (1997).